Int. J. Electrochem. Sci., 14**(2019)** 7529 – 7547, doi: 10.20964/2019.08.65

International Journal of
ELECTROCHEMICAL
SCIENCE
www.electrochemsci.org

Total Phenolic content, Antioxidant and Anticorrosive Activities of *Olea europaea L.* and *Eucalyptus globulus* Cultivated in Tunisian Arid Zones on Steel Rebar's in Alkaline Chloride Solution

Marwa Trimeche[1], *Naceur Etteyeb*[2,3,*], *Abderrahmane Romane*[4], *Mehrez Romdhane*[5]

[1] LR: Energie, Eau , Environnement et procédés, LR18ES35, Faculty of Sciences of Gabes, University of Gabes, Cité Erriadh 6072 Zrig Gabes, Tunisia
[2] High Institue of Applied Biology of Medenine, University of Gabes, km 22,5; Route el Jorf, 4111 Medenine, Tunisia
[3] UR:Eletrochimie, Matériaux et Environnement, UR17ES45, Faculty of Sciences of Gabes, University of Gabes, Cité Erriadh 6072 Zrig Gabes, Tunisia
[4] Cadi AyyadUniversity, Marrakesh, Morocco
[5] LR: Energie, Eau , Environnement et procédés, LR18ES35, National Engineering School of Gabes, University of Gabes, Av. Omar Ibn-Elkhattab 6029, Gabes, Tunisia
[*]E-mail: naceur.etteyeb@gmail.com

Received: 15 December 2018 / *Accepted:* 4 March 2019 / *Published:* 30 June 2019

The aim of this study is to investigate the anticorrosive action of aqueous extracts of some trees *(Olea europaea L.* and *Eucalyptus globulus*) cultivated in Tunisian arid zones on steel rebar's immersed in alkaline chloride medium. Polarization curves, Electrochemical Impedance Spectroscopy (EIS) measurements, Scanning Electron Microscopy (SEM) analyses and the mass loss method at various temperatures and concentration effects were used to carry out the present work. The results obtained from mass loss measurement showed that the inhibition efficiency(%IE) was greatly reduced with the increase of temperature. According to polarization results, the investigated extracts act as a mixed type inhibitor. The EIS results indicated that the corrosion inhibition efficiencies reached a value higher than 90% in the presence of *Olea europaea* rods (OER) extract and 80% of *Eucalyptus globulus* leaves (EGL) extract. SEM analyses of samples in the presence of aqueous extracts revealed the presence of a protective inhibitor layer on the metallic surface, resulting in the protection of steel rebar's from corrosion

Keywords: Alkaline chloride solution; anticorrosive activities; aqueous extracts; carbon-steel; inhibition

1. INTRODUCTION

Steel corrosion was provided with a substantial amount of attention because of its industrial interest [1, 2]. Due to the concrete that provides a very alkaline medium, which leads to the formation of a tightly adhering film and guarantees that the metal remains in the passive state, the protection of the reinforcing steel against corrosion was carried out[3–5]. Passivity was influenced by numerous and well known contaminants, such as chloride ions, which are the localized corrosion triggers, when they hit the surface of the reinforcing steel. In order to reduce the corrosion of rebars, many procedures can be applied [6]. Inhibitors' use is one of the most adapted methods for protecting metals against corrosion [7–12]. However, the used inhibitors are toxic, not friendly to the environment and/or biodegradable, therefore, researchers need to look for cheap and sustainable eco-friendly inhibitors. The use of these clean and cheap plant extracts as green corrosion inhibitors for carbon steel in acidic medium (H_3PO_4, H_2SO_4, HCl) was indicated by several researchers [13, 14, 23–28, 15–22].

To the best of our knowledge, the available data on the use of green inhibitors in alkaline chloride solution are almost limited [1, 5, 7, 29]. The inhibition activities of plant extracts are attributed to the presence of heterocyclic compounds, such as flavonoids, tannins and alkaloids having multiple bonds in their molecule with functional groups containing nitrogen, sulfur and oxygen which improve the formation of protective film over the metal surface [1, 3, 15, 30–32].

The olive (*Olea europaea L.*) and Eucalyptus (*Eucalyptus globulus*) are the most important ever-green trees in Tunisian arid zone. The aim of choosing the Olive Rods (OR) and Eucalyptus Leaves (EL) is intended to provide abundant resources with rapid and continuous renewal, and these organs are supposed to be "waste" and not looked for by animals as a food source. In the current work, we studied the aqueous extracts of *Olea europaea* rods (OER) and *Eucalyptus globulus* leaves (EGL) as inhibitors for corrosion of C-steel (Carbon steel) in interstitial solution of concrete contaminated with chloride ions.

This research study was performed using electrochemical (Polarization and EIS) and analytical (SEM) techniques completed by the mass loss measurements in order to determine the corrosion rate and the inhibition efficiency (%IE) for the concentrations range for EGL and OER.

2. MATERIALS AND METHODS

2.1. Preparation of green inhibitor extract

The main plants used in this research study are *Eucalyptus globulus* and *Olea Europaea*. Fresh olive rods (*OER*) and *Eucalyptus globulus* leaves (*EGL*) were collected in january, 2015 from the region of Medenine, South Tunisia. *EGL* and *OER* are air dried for 30 days in the laboratory at room temperature, crushed and preserved in glass flasks shielded from the light and humidity. Leaves and rods powder (20 g) were extracted by maceration in 200 mL of distilled water. The solutions were taken in continuous magnetic agitation for 3 hours. The extracts were filtered through Whatman no.1 filter paper for removal of particles which are evaporated (T=100°C) by a rotary evaporator. The dry residues are stored at 4°C for later analyses. These solid extracts were used to determine the %IE .

They were dissolved in an aggressive medium that simulates the solution of water/cement (ratio 0.5) and chloride ions (NaCl 3 %) at various concentrations. Before each experiment, we immediately prepared the test solution.

2.2. Determining the content of Secondary metabolites

2.2.1. Determination of Total Phenol Compound

Total phenolic content was performed by using the Folin-Ciocalteu method reported by Germano et al. [33]. Each 0.1 mL of aqueous solution sample was buffered with 0.5 mL of Folin-Ciocalteu reagent was added. We add 4 mL of a solution of sodium carbonate (Na_2CO_3) 1M. The mixture was shaken vigorously and left to stand for 90 min in the dark at room temperature. The reading of the absorbance was made at 765nm using a T60 UV/VIS spectrophotometer. The results were expressed as mg Gallic acid equivalents per g dry weight (mg GA-Eq/ g DW). All tests were done in triplicate.

2.2.2. Determination of Flavonoïds Compound

Total flavonoids content in the extracts was measured following the method of Djeridane et al. [34]. 1 mL of aqueous extract was mixed with 1 ml of Sodium Nitrate solution ($NaNO_2$) 0.5 M and 0.15 mL of Trichloride Aluminum solution ($AlCl_3$) 0.3 M. After incubation of15 min, the absorbance of the reaction mixture was measured at 430 nm. The amount of flavonoids in each extract was expressed as Rutin equivalent in mg per g dry weight (mgR-Eq/ g DW).

2.3. Free radical scavenging activity : DPPH test

In order to evaluate the antioxidant capacitance of plants extracts, we used the 1,1-diphenyl-2-picrylhydrazyl (DPPH) method[35]. The free radical scavenging activities on DPPH test of different extracts were determined according to the method of Okonogie et al. [36]. A test solution of different concentrations was prepared from a stock solution of aqueous extracts (1 mg of dried extract per ml). 100 µM of DPPH was dissolved in distilled water and mixed with an aliquot of 100 µl of each dilution. The mixture was shaken vigorously and incubated for 30 min in the dark at room temperature. The absorbance was read at 517 nm. Results are expressed as the value of the half-maximal effective concentration (EC_{50}) which is defined as the amount of antioxidant necessary to decrease the initial concentration of DPPH at 50%. All measurements were performed in triplicate.

2.4. Working electrode

Corrosion tests were carried out using a carbon steel which is composed of the following percentages (in weight percent): C 0.220%, Fe 99.520%, Mn 0.089%, Si 0.024%, S 0.004%, Ni 0.014%, V 0.016%, Cr 0.009%, Al 0.034%,Cu 0.022%, P 0.046% and Ti 0.003%,and was abraded

with abrasive papers up to 1200 grade. The specimens were washed thoroughly with distilled water then with acetone and air dried at room temperature.

2.5. Electrolyte

The corrosion test solution was a filtrate of water/cement solution (ratio 0.5) added with 3% NaCl called S solution.

2.6. Electrochemical techniques

The potentiodynamic polarization curves were plotted by an AUTOLAB PGSTAT instrument. The surface area of the carbon steel samples, used as the working electrode, was0.18 cm^2. A standard calomel electrode (SCE) was employed as reference electrode. The polarization curves were studied in the potential range ±0.25 mV at a scan rate of 1 mV s^{-1}, the potential was stabilized at free potential during 10 min before all experiments. The linear Tafel segments of anodic and cathodic curves were extrapolated to the corrosion potential to obtain corrosion current densities (j_{corr}). The inhibition efficiency (IE_j %) was determined from the measured j_{corr} values using the following relationship:

$$IE_j\% = \frac{J_{corr}^0 - J_{corr}^{inh}}{J_{corr}^0} \times 100 \quad (1)$$

Where J_{corr}^0 and J_{corr}^{inh} are the corrosion current in the absence and presence of the plants extract, respectively.

The some AUTOLAB equipment was used to determine the Electrochemical Impedance Spectroscopy (EIS) measurements that were performed over a frequency range of 100 kHz to 10 mHz with 7 points per decade at open circuit potential (OCP) using a 10 mV sinusoidal wave amplitude to disrupt the system. The impedance diagrams are given in the Nyquist and Bode representation[37]. The experiments are assessed in triplicate to ensure the reproducibility.

The charge transfer resistance values (R_t) were obtained from the diameter of the semicircles of the Nyquist plots. The inhibition efficiency (IE_{EIS} %) of the inhibitor was obtained from the charge transfer resistance values using the following equation:

$$IE_{EIS}\% = \frac{R_t^{inh} - R_t^0}{R_t^{inh}} \times 100 \quad (2)$$

Where R_t^0 and R_t^{inh} are the charge transfer resistance in the absence and the presence of the plants extract, respectively.

2.7. Analytical techniques: Scanning Electron Microscope (SEM)

The C-steel morphological surfaces after immersion in aggressive solution S of concrete contaminated with chloride ions in the absence or presence of plant extracts at a concentration of $2g.L^1$ were analyzed by scanning electron microscope (SEM).

2.8. Mass loss measurements

Mass loss measurements were carried out under a total immersion in S solution with and without the presence of plants' extracts during 24 hours. The control of the experimental temperature, varied from30 to 60°C,was determined using a water thermostat (±0.1 °C). A steel coupon with an exposed surface area 1.8 cm² was used. The corrosion rate (*W*) was calculated as:

$$W = \frac{\Delta M}{s \times t}(mg.cm^{-2}.h^{-1}) \quad (3)$$

where ΔM represents the mass loss of carbon steel (mg), S is the exposed area of the coupon (cm^2) and t is the exposure time (h). The experiments were performed in triplicate and the average value of the mass loss was noted.

The percentage of inhibition efficiency was calculated using the following equation:

$$IE_W\% = \frac{W - W_i}{W} \times 100 \quad (4)$$

where W and W_i are the corrosion rates of the steel coupons in the absence and presence of plant extracts, respectively.

2.9. Statistical Analyses

Statistical analyses were performed using GLM procedure performed by SPSS 20 software. The Two-way ANOVA was conducted to compare the data between OER and EGL. Differences at $p < 0.05$ were considered statistically significant by SNK (Student Newman Keuls) test. All samples were analyzed in triplicate.

3. RESULTS AND DISCUSSION

3.1. Total phenols and Flavenoids contents

Table 1 indicates the results obtained from the determination of total phenols and flavenoids contents. The values are the average of three repetitions.

Results show that with the *Eucalyptus globulus leaves* (EGL) extract we obtained the highest values of total polyphenols and flavenoids. As shown in Table 1, the total polyphenols, expressed as mg Gallic Acid equivalents per g dry weight(mg GA-Eq/ g DW), had the most elevated amount in EGL (275.1±16.54 mg GAE/ g DW) followed by OER (108.5±14.19 mg GA-Eq/ g DW). Total flavenoids are 22.68±0.99 and 6.47±0.52 mg Rutin equivalents per g dry weight (mg R-Eq/ g DW) for EGL and OER, respectively.

While, Amamra et al. are investigated *Thymus vulgaris* aqueous extracts as green corrosion inhibitor and found that this plant contains a lower level of secondary metabolites than our plant extracts : The total polyphenols and flavonoids contents were 97.11±2.83 mg GA-Eq/ g DW and 12.55±0.22[35]

According to the results presented in Table 1, it was found that the different extracts obtained from the extraction of phenols with an aqueous solvent (distilled water) contained acceptable quantities

of natural antioxidants. Moreover, these results encourage to look for the possibility to enhance the extraction of natural antioxidants using water and avoid organic solvent.

Table 1. Mean values of total polyphenols, flavenoids and DPPH radical scavenging activities of EGL and OER aqueous extracts

	Total plyphenols (mgGA-Eq/ g DW)	*Flavenoids (mg R-Eq/ g DW)*	*DPPH (EC50) (µL/mL)*
EGL aqueous extract	275.1±16.54	22.68±0.99	12.22±0.05
OER aqueous extract	108.5±14.19	6.47±0.52	25.48±0.59

3.2. Antioxidant activity : DPPH

DPPH is a free radical compound that has been widely used to determine the free radical-scavenging ability of various samples [38]. The free radical scavenging activity was expressed as the EC50 value (the effective concentration of extract required to inhibit 50% of the initial DPPH free radical). Results reported in Table 1, show that both aqueous extracts displayed good antioxidant activities. The EC50 value of OER (25.48 ±0.59 µg/mL) was higher than EGL (12.22 ±0.05 µg/mL). According to these values , the current study is in agreement with previous studies reporting high DPPH radical scavenging activity of EGL compared to OER. These may be related to the richness of EGL with different types of phenols [29]. These results proposes that polyphénols and flavonoids are the major responsible of the antioxidant activity .

3.3. Electrochemical results

3.3.1. Behaviour of the open circuit potential

We first thought that it was important to know the evolution of the open circuit potential vs. time of the carbon steel immersed in a corrosive S solution without and with *EGL* and *OER* aqueous extracts at various concentrations. The results obtained are presented in Fig. 2 (A) and (B), respectively.

In the absence of the green-inhibitor "control curve", it was found that the values of the free potential (E_{corr}) gradually tend towards the cathodic direction and become stable over time. There is a continuous attack of metal, then the stability of the free potential shows that the oxidizing/reducing systems involved in the corrosion phenomena are the similar kinetics.

For all experiments conducted in the presence of *EGL* or *OER* extracts, a displacement of the corrosion potential towards the positive values was observed. This shift is more pronounced in the experiments performed with a 1.5 or 2 $g.L^{-1}$ concentration. This variation of potential indicated a significant change in the metal/solution interface and indicated that the system is protected by a protective layer formation which contains the oxidation products that have reacted chemically with the

constituents of the corrosive medium. This behaviour highlights a passivation phenomenon. The overall results demonstrated that the extract acts preferentially on the anode process.

The initial decrease in the potential observed in the presence of *EGL* or *OER* extracts can be attributed to the dissolution of the native oxide formed on the electrode surface during the transfer of the sample between the polishing and the electrochemical cell.

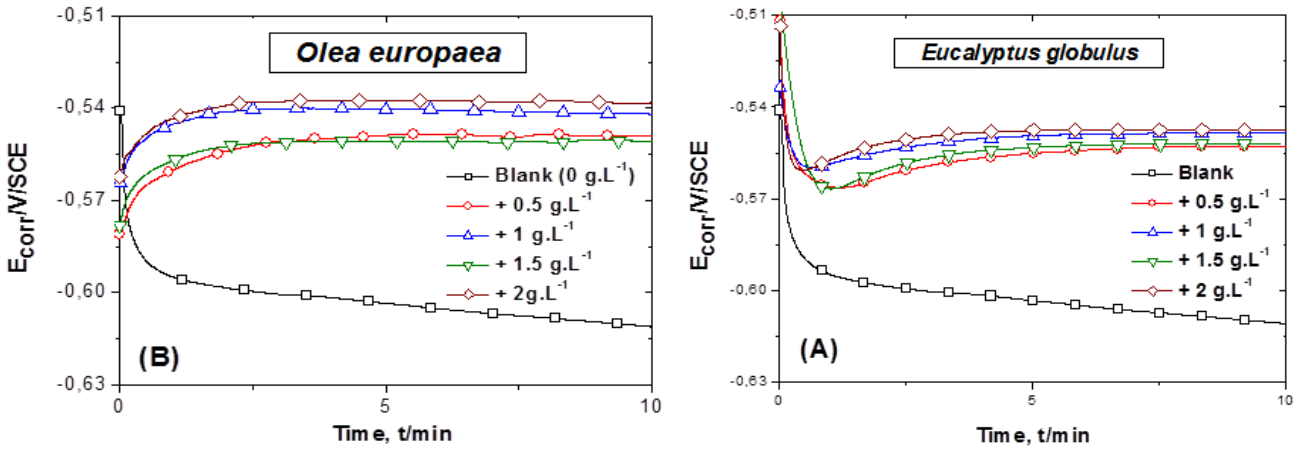

Figure 2. Open circuit potential vs. time of the carbon steel immersed in aggressive S solution (filtrate of water/cement solution (ratio 0.5) added with 3% NaCl) without and with (A) *Eucalyptus globulus* extract, (B) *Olea europaea* extract, at various concentrations (0.5; 1; 1.5 and 2 $g.L^{-1}$).

3.3.2. Polarisation curves: j = F (E)

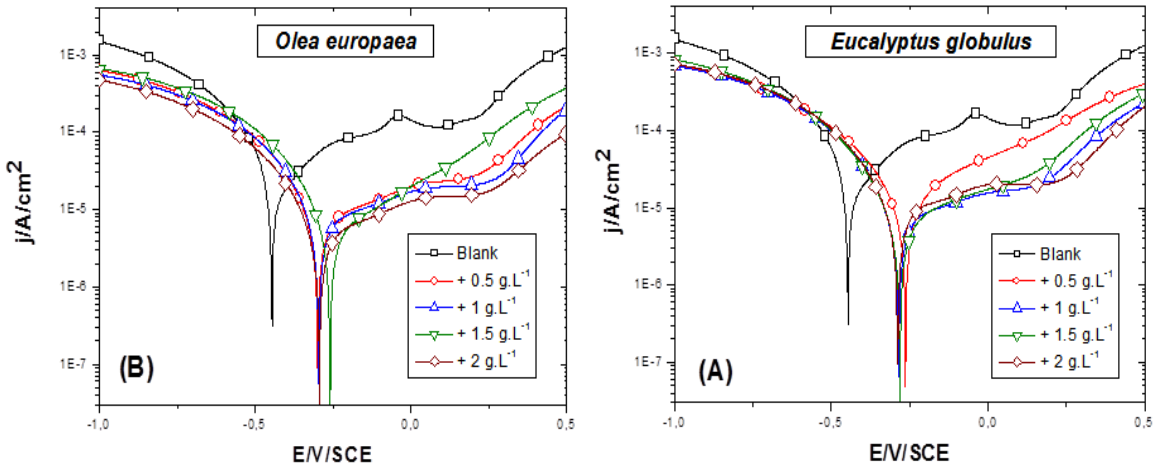

Figure 3. Polarisation curves of the carbon steel immersed in aggressive S solution (filtrate of water/cement solution (ratio 0.5) supplemented with 3% NaCl) without and with (A) *Eucalyptus globulus* extract, (B) *Olea europaea* extract, at various concentrations (0.5; 1; 1.5 and 2 $g.L^{-1}$).

The polarization curves were plotted after 10 min of immersion of the working electrode in the corrosive S Solution. The potential range varies from -1V to + 0.5V with an arbitrarily scanning speed $1mV.s^{-1}$.

Figs. 3 (A) and (B) show the polarization curves of the carbon steel immersed in the S solution without and with the addition of *EGL* or *OER* at various concentrations, respectively.

A slight decrease of the cathodic current density was noted for all experiments performed in the presence of plants extract, however itresulted also in a significant decrease of the current density in the anode region. It seems that the *EGL* or *OER* extracts changes completely the reaction of steel dissolution and reinforces the passive state of the electrode.

From these curves, electrochemical parameters characteristic (E_{corr}, β_a, β_c, j_{corr} and IE_j) were determined. They are reported in Table 2. The percentage of inhibition efficiency (IE_j%) was calculated according to equation 1.

Table 2. Kinetic parameters determinated from the polarization curves presented in Fig. 3

C/g.L^{-1}		β_a/mV dec^{-1}	β_c/mV dec^{-1}	E_{corr}/V$_{SCE}$	j_{corr}/µA cm^{-2}	η *(%)*
Blank	0	68.3	-241.7	-0.451	23.7	-
EGL	0.5	47.4	-218.6	-0.286	5.76	75.7
	1	43.2	-203.4	-0.285	5.31	77.6
	1.5	40.1	-205.1	-0.287	4.85	79.5
	2	35.7	-173.7	-0.267	3.52	85.2
OER	0.5	49.4	-217.2	-0.296	4.24	82.1
	1	41.8	-205.7	-0.295	3.34	85.9
	1.5	34.6	-201.2	-0.297	3.25	86.3
	2	32.2	-184.3	-0.258	2.05	91.4

Comparing the electrochemical behaviour of the carbon steel in neutral chloride medium in the vicinity of the corrosion potential without and with addition of the *EGL* or *OER* extract shows that:

- The corrosion current density decreases significantly with the addition of *EGL* or *OER*extract. This, of course, reflects the formation of the protective layer on the metal surface that prevents corrosion. However, the lower density is observed with the presence of *EGL* or *OER* extract at a rate ≥ 1.5 g.L^{-1}.
- The inhibitory efficiency evolves in the same way and reaches a maximum value of 91.2% in the presence of *OER* extract with an amount of a 2 g.L^{-1}.

3.3.3. Electrochemical Impedance Spectroscopy (EIS)

Electrochemical impedance spectroscopy technique was used in order to confirm the results obtained by the stationary electrochemical methods.

Figures 4 and 5 show the impedance diagram in the Nyquist and Bode plane of carbon steel immersed in a corrosive S solution with and without the addition of the *EGL* or *OER* extract at various concentrations, respectively. These diagrams were recorded after 10 min of maintaining the open circuit potential in a frequency ranged between 100 kHz and 10 mHz.

The impedance diagrams obtained are not perfect semi-circles, and this can be due to the dispersion of the frequency of the interfacial impedance[28, 39, 40],generally caused by the heterogeneity of the electrode surface. This latter can result in roughness, dislocations, impurities, the inhibitor adsorption, and the formation of porous layers[41–43].

It appears that the total impedance increases with the increase of the plant extracts concentration.

These diagrams show a capacitive behavior of the interface in the considered frequency range. They are formed of two loops: the first in the high frequencies range is attributed to the charge transfer while the second which is on the low frequency range is relative to the adsorption of the inhibitory molecules on the metal surface and all other products accumulated in the metal/solution interface (corrosion products, molecules of inhibitor, etc.)[44].

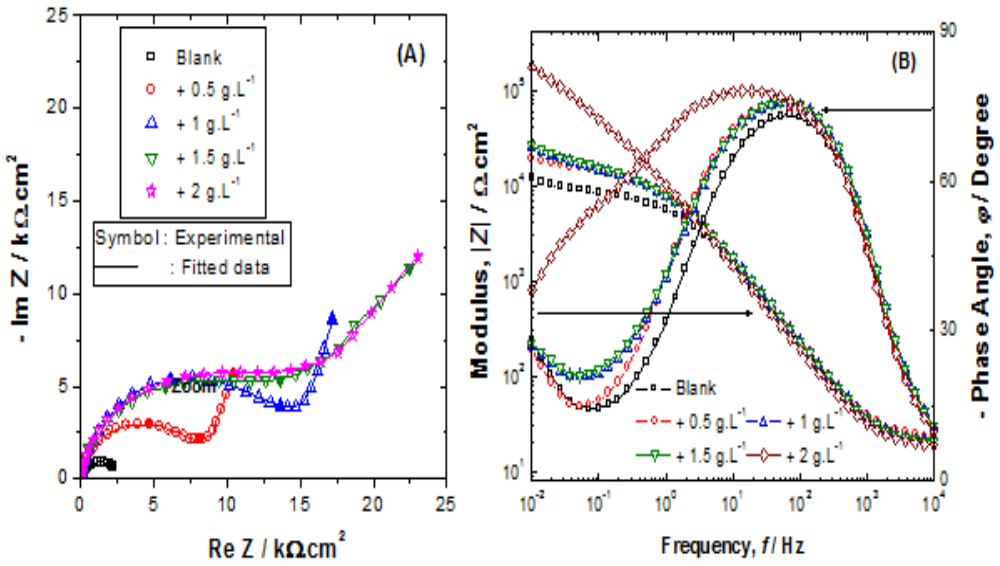

Figure 4. Electrochemical impedance spectrum of carbon steel immersed in the aggressive S solution (filtrate of water/cement solution (ratio 0.5) supplemented with 3% NaCl) without and with *Eucalyptus globulus* leaves extract at various concentrations; (A) Nyquist plane, (B) Bode plane.

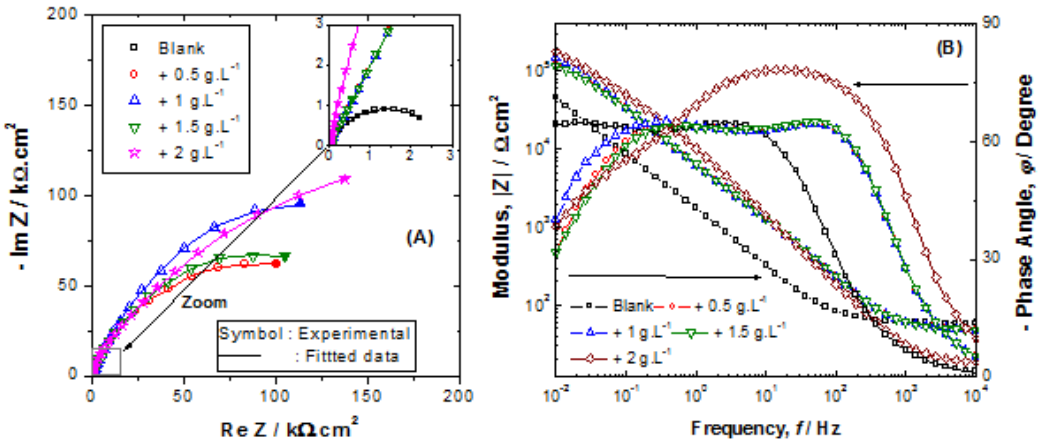

Figure 5. Electrochemical impedance spectrum of carbon steel immersed in the aggressive S solution (filtrate of water/cement solution (ratio 0.5) supplemented with 3% NaCl) without and with *Oleaeuropaea* rods extract at various concentrations; (A) Nyquist plane, (B) Bode plane.

For more detailed analysis and further discussion of the change in impedance diagrams, the results of the EIS were modeled with an equivalent electrical circuit. In all EIS spectra, there is a depressed semi-circle; such behaviour can be explained as a deviation from the ideal capacity. Therefore, a constant phase element(*CPE*) was used in the proposed circuit.

Therefore, the equivalent circuit used in this work consists of an arrangement of elements hierarchically distributed (Fig. 6) depending on the impedance function given by equation (5) [5, 45].

$$Z_{CPE} = Q^{-1}(j\omega)^{-\alpha} \quad (5)$$

where Q defined the *CPE* constant, ω is the angular frequency in rad s^{-1} and $j = (-1)^{1/2}$ is the imaginary number. The interpretation of these elements depends on the α value.

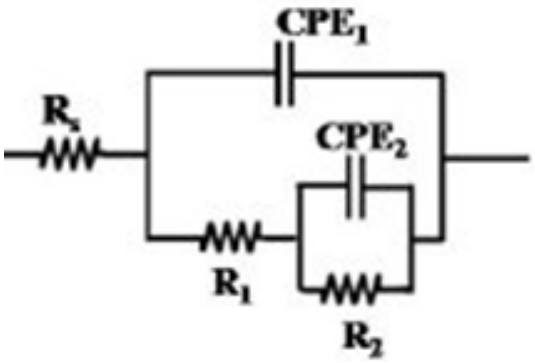

Figure 6. Equivalent circuit used to fit all Impedance spectra's

Fig. 7 shows the values of the charge transfer resistance, $R_t(R_1)$, derived from impedance spectra of Figs. 3 and 4.

By analyzing these results, we can draw the following remarks:

- The R_t values increase considerably with the rise of the plant material concentration.

This result shows the inhibitory effect of the extract.

- A maximum inhibitory efficacy of 95% is obtained in the presence of *OER* aqueous extract at a rate of 2 $g.L^{-1}$.

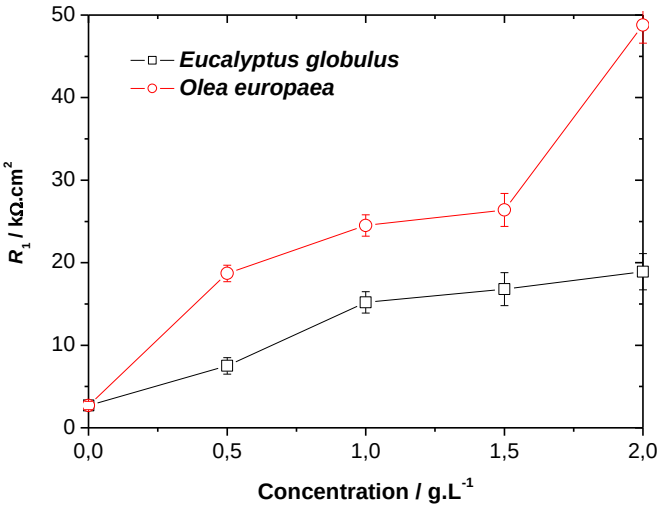

Figure 7. Evolution of R_1 versus time of carbon steel immersed in the aggressive S solution (filtrate of water/cement solution (ratio 0.5) added with 3% NaCl) without and with plant extract

The results achieved by EIS are in good agreement with those realized by stationary electrochemical techniques (corrosion potential and polarization curves).

3.4. Analytical results

3.4.1. Scanning electron microscopy (SEM)

Scanning electron microscopy (SEM) micrograms of the polished surface of carbon steel immersed in aggressive S solution in the absence and presence of the *EGL* and *OER* extracts at a concentration of 2g.L^{-1} were shown in Fig. 8(a), (b) and (c), respectively.

For blank specimens (Fig. 8 a), a rough surface caused by the attack of the corrosive medium on the carbon steel surface and formation of a rust product on the surface was noticed. Whereas, in the presence of plant extracts (Figs. 8 b and c), the carbon steel surface became smooth.

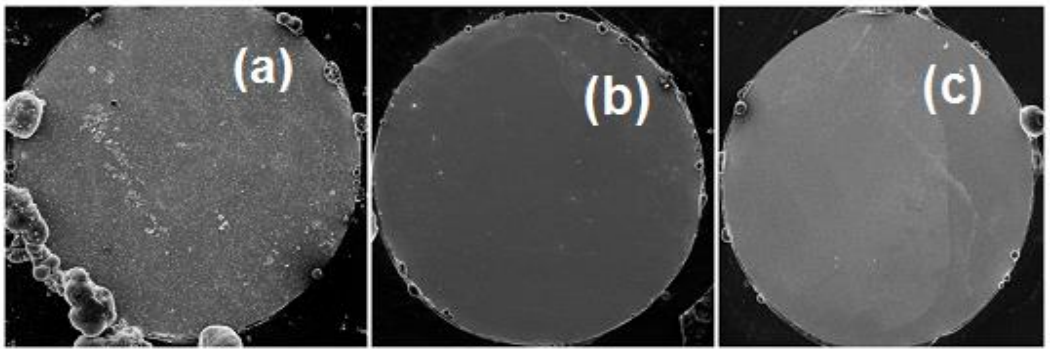

Figure 8. SEM surface morphologies of the carbon steel immersed in the aggressive S solution (filtrate of water/cement solution (ratio 0.5) added with 3% NaCl) (a). Effects of the addition of the aqueous extract of: *Eucalyptus globulus* leaves (b) and *Olea europaea* rods (c).

3.5. Mass loss results

A gravimetric method (mass loss measurement) was applied to evaluate the corrosion inhibition of steel in alkaline chloride solution using the *Eucalyptus* and *Olive* extracts, due to its high reliability and simple application[21].

3.5.1. Effect of green inhibitor on corrosion rate

A weight loss method at a temperature ranging from 30°C to 60°C was used to determine the corrosion rate of C-steel in different concentrations (0-2 g L^{-1}) of aqueous extracts for an exposure time of 24 hours. It is observed that C-steel corrodes at different concentrations of aqueous extract. The C-steel corrodes in alkaline chloride medium with the decrease in original weight of C-steel. Air, water, and hydrogen ion are the major effects of the corrosion process which takes place at the surface of C-Steel. The corrosion rate decreased with the increase of *EGL* extract concentration in alkaline chloride solution as shown in Fig.9.This behavior can be argued by the formation of a protective film which is more resistant and adherent on the surface of C-steel. The same results were achieved when using the *OER* extract (Fig. 10).The formation of a protective layer of ferric hydroxide on the C-steel surface occurred when the extract concentrations increase and the corrosion rates decrease[46].A further increase in temperature from 30°C to 40°C decreases the corrosion rate. This can be due to the formation of ferric hydroxide layer on the C-steel surface which dissolves at the rise of temperature from 40°C to 60°C. Then, at a temperature ranging from 40°C to 60°C the corrosion rate increases. These results show that *EGL* and *OER* extracts act as an effective inhibitor in the range of temperature studied.

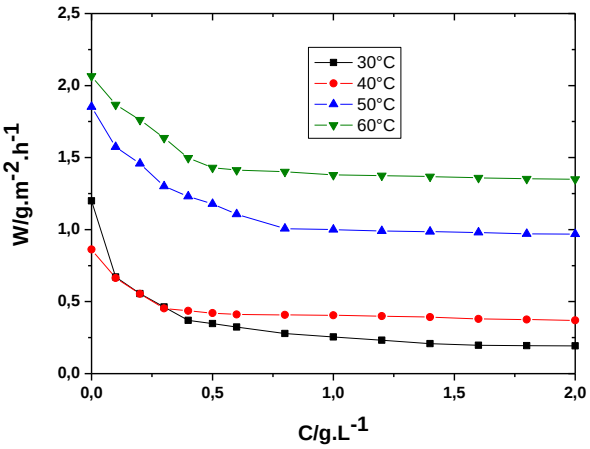

Figure 9. Relationship between the corrosion rate (*W*) of C-steel and the concentration of *EGL*

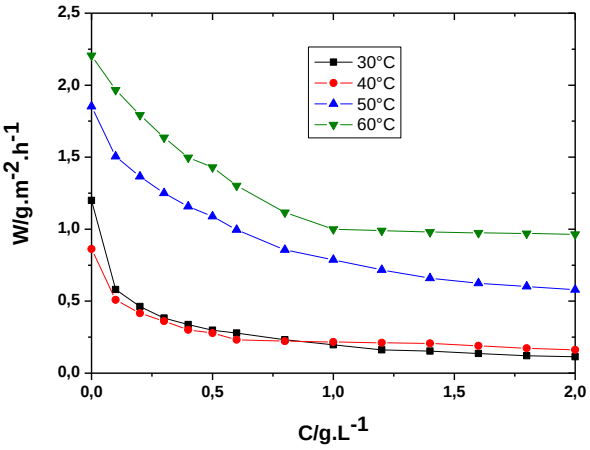

Figure 10. Relationship between the corrosion rate (*W*) of C-steel and the concentration of *OER*

3.5.2. Effect of green inhibitor on inhibition efficiency

Figs. 11 and 12 present the values of IE% for different concentrations of alkaline chloride solution without and with *EGL* and *OER* at 30–60°C on C-Steel. The *IE*% increases with the inhibitor concentration for both EGL and OER extracts. At the inhibitor concentration of 2.0 g L^{-1}, the maximum of *IE*% for *OER* extract is 90.55% at 30°C; 81.21% at 40°C; 68.75% at 50°C; and 56.27% at 60°C. However, for *EGL* extract, the values are 83.99% at 30°C; 57.11% at 40°C; 47.70% at 50°C; and 34.63% at 60°C. The obtained results demonstrated that *EGL* and *OER* extracts are an effective inhibitor for C-steel in the alkaline chloride solution. Figs. 11 and 12 also show that increasing in temperature leads to a decrease of inhibitive ability, which proved that the desorption of inhibitor from the C-steel surface may be due to the higher temperature.

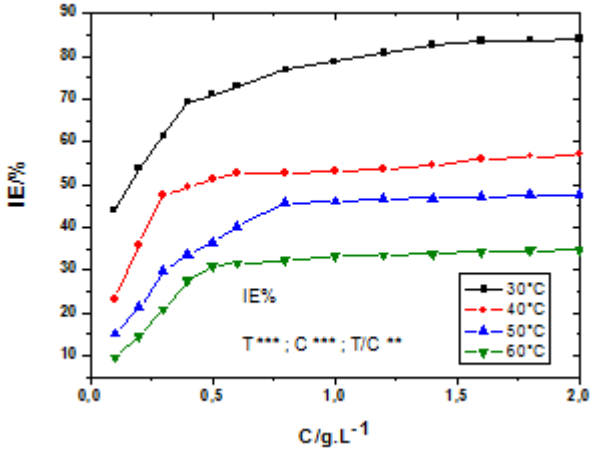

Figure 11. Relationship between the inhibition efficiency (*IE*) of C-steel and the concentration of *EGL*

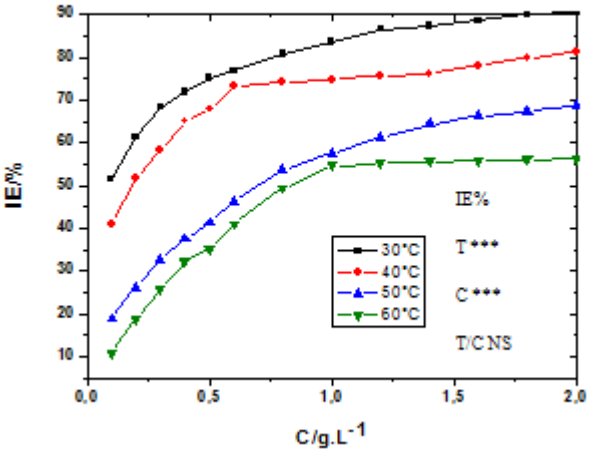

Figure 12. Relationship between the inhibition efficiency (*IE*) of C-steel and the concentration of *OER*

*Significant differences were designed according to p values by : p<0.05: *; p<0.01: **; p<0.001:*** and p > 0.05: NS (not significant)*

The inhibition efficiency (IE%) varied significatly (*p<0.01*) under the effects of temperature (T), concentration (C) and their interaction (T/C) for both EGL and OER.

3.5.3. Adsorption behaviour

The corrosion of the C-steel could be due to the adsorption of the components of the green inhibitors on the surface because of the inhibitory actions of the extracts, and some adsorption isotherms were widely used to study the adsorption behavior. The decrease in the corrosion rate is related to the adsorbed layer which acts as a barrier between the steel surface and the aggressive solution. It indicates that the inhibition efficiency (*IE*) is proportional to the fraction of the surface covered by the adsorbed molecules (θ). As a result, (θ) is calculated using the relation $\theta = \frac{IE}{100}$ and the calculated values are shown in Table 3. In this study, the adsorption of *EGL* and *OER* extracts on C-steel surface obeys Langmuir adsorption isotherm [47] : $\frac{C}{\theta} = \frac{1}{k} + C$ where *C* is the concentration of inhibitor, *K* is the adsorptive equilibrium constant. A straight line, with a slope and linear correlation coefficients (*r*) close to 1, is obtained when the extract concentration (C) is plotted against C/θ at different temperatures (Figs. 13 and 14).This behavior suggests that the *OER* and *EGL* adsorbed onto C-steel surface following the Langmuir adsorption isotherm. As indicated in Table 3, the adsorptive equilibrium constant (*K*) decreases as the temperature is increased for both *EGL* and *OER* aqueous extracts. This may be associated with the easy adsorption of the inhibitor onto the C-steel surface at lower temperature. Moreover, at certain temperatures, K (*OER*) > K (*EGL*) meaning that *OER* provided the strongest adsorptive tendency on C-steel surface. These results are in accordance with the values of inhibition efficiency obtained from Figs. 11 and 12.

Table 3. Parameters of the linear regression between *C/θ* and *C* in alkaline chloride solution

Extract	Temperature (°C)	R	Slope	K (L g^{-1})
OER	30	0.9909	1.047	7.7519
	40	0.9975	1.178	6.8493
	50	0.9995	1.182	1.8382
	60	0.9995	1.347	1.5873
EGL	30	0.9949	1.116	7.0922
	40	0.9975	1.670	5.3763
	50	0.9995	1.830	2.2624
	60	0.9995	2.541	1.7331

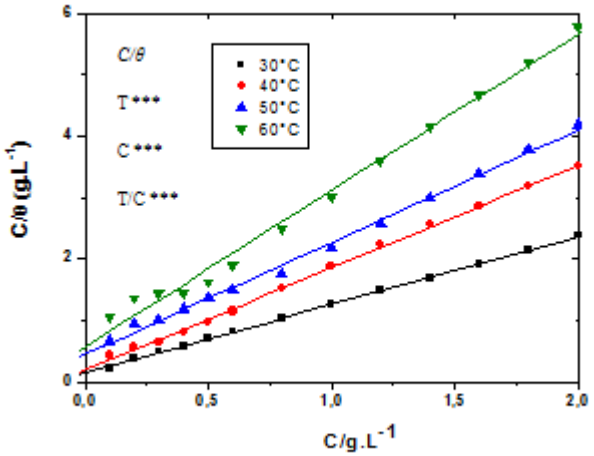

Figure 13. Langmuir isotherm adsorption mode of *EGL* on C-steel surface in alkaline chloride solution. Significant differences were designed according to *p* values by :$p<0.05$: *; $p< 0.01$:* *; $p<0.001$:*** and $p> 0.05$: NS (not significant)

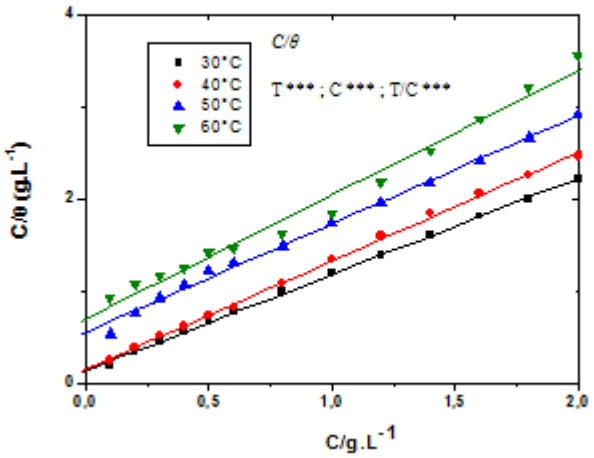

Figure 14. Langmuir isotherm adsorption mode of *OER* on C-steel surface in alkaline chloride solution. The value of *C/θ* varied significatly ($p<0.01$) under the effects of temperature (T), concentration (C) and their interaction (T/C) except for the effect (T/C) on *EI%* analyses for OER.

3.5.4. Thermodynamic parameters

Thermodynamic parameters are effective to understand the adsorption process of the inhibitor on C-steel/alkaline chloride solution interface. *ΔH°*, the standard adsorption enthalpy, may be calculated from the Van't Hoff equation:

$$\frac{d\ln k}{dT} = \frac{\Delta H^0}{RT^2} \quad (6)$$

where *R* is the gas constant (8.314 J K^{-1} mol^{-1}), T the absolute temperature (*K*), and *K* is the adsorptive equilibrium constant. Equation (6) can be written as follows:

$$\ln k = -\frac{\Delta H^0}{RT} + D \quad (7)$$

where D is an integration constant. ΔH° is determined from the slope of Lnk versus 1/T curve for the *EGL* and *OER* (the linear correlation coefficients are 0.937 and 0.974 for *EGL* and *OER*, respectively), and listed in table 4.

The adsorptive equilibrium constant (*K*) is linked to the standard adsorption free energy (*ΔG°*) obtained by:

$$k = \frac{1}{C_{solvent}} \exp(-\frac{\Delta G^0}{RT}) \quad (8)$$

where $C_{solvent}$ is the concentration of water in the solution. We noted that the $C_{solvent}$ unit can be found in that of *K*. As indicated in table 2, the unit of *K* is $L.g^{-1}$, which leads to the unit of $C_{solvent}$ is $g.L^{-1}$ with the approximate value 1.0×10^3. To find the value of the standard adsorption entropy (*ΔS°*), the following thermodynamic basic equation should be used:

$$\Delta S^0 = \frac{\Delta H^0 - \Delta G^0}{T} \quad (9)$$

where all the standard thermodynamic parameters are provided in table 4.

The negative value of *ΔH°* demonstrated the exothermic nature of the process for the adsorption of inhibitor over the entire metal surface, which suggests that rise in the temperature resulted in the desorption amount of some adsorbed inhibitor molecules from the C-steel surface. The calculated values of *ΔG°* are around -20 kJ mol^{-1}, which can be explained by the adsorption of plant extracts on the C-steel surface belongs to the physisorption [48]:The negative sign shows that the adsorption of *EGL* and *OER* extracts onto C-steel surface is a spontaneous process, and suggests the stability of the adsorbed layer on the C-steel surface, which leads to a strong physical adsorption. It is well known that the free energy of adsorption values are of the order of -20 kJ mol^{-1} which implies an electrostatic interaction between the charged molecules and the dissimilar charge metal, while those of -40 kJ mol^{-1} involve charge sharing or a transfer of electron from the green inhibitor molecules to the C-steel surface to provide a coordinate type of bond (chimisorption).

Table 4. Standard thermodynamic parameters of the adsorption of green inhibitor extract on C-steel surface in alkaline chloride solution

Extract	Temperature (K)	$\Delta G°$ (kJ mol^{-1})	$\Delta H°$ (kJ mol^{-1})	$\Delta S°$ (J mol^{-1} K^{-1})
EGL	303	-22.56	-50.5	-92
	313	-22.98	-50.5	-88
	323	-20.19	-50.5	-94
	333	-20.40	-50.5	-90
OER	303	-22.34	-42.3	-66
	313	-22.35	-42.3	-64
	323	-20.74	-42.3	-67
	333	-20.65	-42.3	-65

Table 4 shows that the signs of entropy ($\Delta S°$) are negative for both extracts which implies that the activation complex in the rate determining step represents an association rather than dissociation step. This implies that the activated inhibitor molecules are in a higher order state compared to the initial ones. Moreover, the negative value of $\Delta S°$ means that the inhibitor adsorption is accompanied by a lower desorption of water molecules from the surface (bi-molecular process).

4. CONCLUSION

1. Eucalyptus leaves and olive rods extracts are a good eco-friendly inhibitor for carbon steel in alkaline chloride solution and may be used to substitute toxic chemicals.
2. The effectiveness of inhibition (*IE*%) decreases with the increase of the temperature and rises with the concentrations of inhibitor. The *IE*% in the presence of *OER* aqueous extract at 2 g L^{-1} reached a value higher than 90%.
3. The introduction of inhibitor extracts into the alkaline chloride medium leads to the formation of a film on the C-steel surface which effectively protects the steel from corrosion. The surface photographs showed a good surface coverage on the C-steel surface in the presence of plant extracts.
4. The results obtained from various corrosion techniques emphasize that the corrosion rate of C-steel increase with temperature, suggesting that the adsorption of *OER* and *EGL* on C-steel surface is a physisorption type and obeys Langmuir isotherm.
5. The inhibition efficiency values obtained from weight loss method, polarisation, EIS and SEM techniques are in good agreement.

ACKNOWLEDGEMENTS

The authors are grateful to Dr. Walid ELFALLEH from the Higher Institute of Applied Sciences and Technology of Gabes for his advice and technical support , as well as Miss Amina GAMMOUDI from the Higher Institute of Applied Biology of Medenine for providing language help. The authors are also grateful to the Ministry of Higher Education and Scientific Research, Tunisia, for the financial support.

References

1. M. A. Ameer, A. M. Fekry, A. A. Ghoneim, and F. A. Attaby, *Inter.J.Electrochem. Sci.,5* (2010) 1847.
2. M. B. Valcarce and M. Vázquez, *Electrochim. Acta* ,53 (2008) 5007.
3. M. A. Ameer and A. M. Fekry, *Inter.J.Hydrogen Energy* ,35 (2010) 11387.
4. M. B. Valcarce and M. Vázquez, *Mater.Chem.Phys.,115* (2009) 313.
5. L. Freire ,M. J. Carmezim ,M. G. S. Ferreira and M. F. Montemor,*Electrochim. Acta*,56 (2011) 5280.
6. L. Dhouibi, E. Triki, and A. Raharinaivo, *Cem.Concr.Compos.*, 24 (2002) 35.
7. N. Etteyeb, L. Dhouibi, H. Takenouti, M. C. Alonso, and E. Triki, *Electrochim. Acta*, 52 (2007) 7506.
8. N. Etteyeb, M. Sanchez, L. Dhouibi, M. C. Alonso, H. Takenouti, and E. Triki, *Corros.Eng. Sci. Technol.,45* (2010) 435.
9. N. Etteyeb, L. Dhouibi, H. Takenouti, and E. Triki, *Cem.Concr. Compos.*, *55* (2015) 241.
10. J. J. Shi and W. Sun, *Cem.Concr.Compos.,45* (2014) 166.
11. D. M. Bastidas, M. Criado, S. Fajardo, A. La Iglesia, and J. M. Bastidas, *Cem.Concr.Compos.*, 61 (2015) 1.
12. A. Fawzy, *Inter.J.Electrochem. Sci.*,14 (2019) 2063.
13. N. M'hiri, D. Veys-Renaux, E. Rocca, I. Ioannou, N. M. Boudhrioua, and M. Ghoul, *Corros. Sci.*,102 (2016) 55.
14. A. Y. El-Etre, M. Abdallah, and Z. E. El-Tantawy, *Corros. Sci.*, 47 (2005) 385.
15. X. Li and S. Deng, *Corros. Sci.*, 65 (2012) 299.
16. M. Tezeghdenti, N. Etteyeb, L. Dhouibi, O. Kanoun, and A. Al-Hamri, *Prot.Met.Phys.Chem. Surfaces*, 53 (2017) 753.
17. J. C. da Rocha, J. A. da Cunha Ponciano Gomes, and E. D'Elia, *Corros. Sci.*, 52 (2010) 2341.
18. M. Lebrini, F. Robert, A. Lecante, and C. Roos, *Corros. Sci.*,53 (2011) 687.
19. P. Mourya, S. Banerjee, and M. M. Singh, *Corros. Sci.*, 85 (2014) 352.
20. A. M. Fekry and M. A. Ameer, *Inter.J. Hydrogen Energy, 35* (2010) 7641.
21. D. Bouknana, B. Hammouti, H. Serghini caid, S. Jodeh, A. Bouyanzer, A. Aouniti, and I. Warad, *Inter.J. Ind.Chem., 6* (2015) 233.
22. L. Li, X. Zhang, J. Lei, J. He, S. Zhang, and F. Pan, *Corros. Sci.*, 63 (2012) 82.
23. X. Li, S. Deng, X. Xie, and H. Fu, *Corros. Sci.*, 87 (2014) 15.
24. X. Li, S. Deng, and H. Fu, *Corros. Sci.*, 62 (2012) 163.
25. Z. V. P. Murthy and K. Vijayaragavan, *Green Chem.Let.Rev.*,7 (2014) 209.
26. G. Ji , S. Anjum,S. Sundaram and R. Prakash, *Corros. Sci.*,90 (2015) 107.
27. V. Torres, V. Rayol, M. Magalhães,G. Viana,L. Aguiar,S. Machado, H. Orofino and E. D'Elia, *Corros. Sci.*, 79 (2014) 108.
28. L. Boucherit, T. Douadi , N. Chafai, M. Al-Noaimi, S. Chafaa, *Inter.J.Electrochem. Sci.*,13 (2018) 3997.
29. N. Etteyeb and X. R. Nóvoa, *Corros. Sci.*, 112 (2016) 471.
30. O. Benali, H. Benmehdi, O. Hasnaoui, C. Selles and R. Salghi, *J.Mat.Envir.Sci.*,4 (2013) 127.
31. P. Raja, A. Qureshi ,A. Abdul Rahim, H. Osman and K. Awang, *Corros. Sci.*,69 (2013) 292.
32. A. Fawzy, M. Abdallah, M. Alfakeer and H. M. Ali, *Int. J. Electrochem. Sci.*,14(2019) 2063.
33. M. P. Germano, R. De Pasquale, V. D'Angelo, S. Catania, V. Silvari, and C. Costa, *J. Agric.Food Chem.*, 50 (2002) 1168.
34. A. Djeridane, M. Yousfi, B. Nadjemi, D. Boutassouna, P. Stocker, and N. Vidal, *Food Chem.*, *97* (2006) 654.
35. S. Amamra, M. E. Cartea, O. E. Belhaddad, P. Soengas, A. Baghiani, I. Kaabi and L. Arrar,*Int. J. Electrochem. Sci.*,13 (2018) 7882.

36. S. Okonogi, C. Duangrat, S. Anuchpreeda, S. Tachakittirungrod, and S. Chowwanapoonpohn, *Food Chem.,103* (2007) 839.
37. M. Tezeghdenti, L. Dhouibi and N. Etteyeb, *J.Bio-,Tribo-Corrosion*, 1 (2015) 16.
38. R. Amarowicz, R. B. Pegg, P. Rahimi-Moghaddam, B. Barl, and J. A. Weil, *Food Chem.,* 84 (2004) 551.
39. S. Martinez and M. Metikoš-Huković, *J.Appl.Electrochem.,* 33 (2003) 1137.
40. M. Elayyachy, A. El Idrissi, and B. Hammouti, *Corros. Sci.,* 48 (2006) 2470.
41. P. Li, J. Y. Lin, K. L. Tan, and J. Y. Lee, *Electrochim. Acta,* 42 (1997) 605.
42. Z. Stoynov, *Electrochim.Acta,* 35 (1990) 1493.
43. A. Yurt, S. Ulutas, and H. Dal, *Appl.Surf.Sci.,* 253 (2006) 919.
44. A. Zarrouk, H. Zarrok, Y. Ramli, M. Bouachrine, B. Hammouti, A. Sahibed-dine and F. Bentiss, *J. Mol. Liq.*,222 (2016) 239.
45. L. Yohai, M. Vázquez, and M. B. Valcarce, *Electrochim.Acta,* 102 (2013) 88.
46. D.B. Patil and A.R. Sharma,*E-J. Chem.*,8 (2011) 358.
47. R. F. V. Villamil, P. Corio, S. M. L. Agostinho, and J. C. Rubim, *J. Electroanal.Chem.,* 472 (1999) 112.
48. Y. Abboud, O. Tanane, A. El Bouari,R. Salghi,B. Hammouti, A. Chetouani and S.Jodeh, *Corros.Eng. Sci.Tech.,* 50(2015)557.